Supplementary Material

Accurate and noninvasive diagnosis of the epithelial cancers through AND gate photoluminescence on tumor-derived small extracellular vesicles

Nanhang Zhu [a], Xuekang Wang [a], Xingyou Wang [a], Yating Zeng [a], Yue Yu [a], Qiangying Yi [a] *, Yao Wu [a] *

[a]National Engineering Research Center for Biomaterials, Sichuan University, Chengdu 610064, P. R. China

Corresponding Author:

**E-mail: qyi@scu.edu.cn (Q.Y.).*

**E-mail: wuyao@scu.edu.cn (Y.W.).*

Tab. S1 Detailed information of aptamer sequences and modifications.

Name	Sequence (5' to 3')	Modification
Apt_{EpCAM}	CAC TAC AGA GGT TGC GTC TGT CCC ACG TTG TCA TGG GGG GTT GGC CTG	3`SH C6
Apt_{MUC1}	TTTTTTTTTGCAGTTGATCCTTTGGATACCCTGG	5`NH_2 C6
temP	CCAGGGTATCCAAAGGATCAACTGCAAAAAAAAACAGGCCA ACCCCCCATGACAACGTGGGACAGACGCAACCTCTGTAGTG	

Tab. S2 Information of clinical samples.

No.	Cancer Type	Gender	Age	Diagnosis Information
B1	Breast	Female	50	None ductal carcinoma in situ with invasive carcinoma
B2	Breast	Female	48	Invasive ductal carcinoma
B3	Breast	Female	85	Invasive ductal carcinoma
B4	Breast	Female	67	Invasive ductal carcinoma
B5	Breast	Female	50	Invasive ductal carcinoma
B6	Breast	Female	69	Invasive ductal carcinoma
T1	Lung	Female	49	Malignant lung tumor
T2	Liver	Female	69	Hepatocellular carcinoma
T3	Liver	Female	57	Metastatic hepatocellular carcinoma
T4	Liver	Female	49	Liver cancer/cirrhosis of the liver
T5	Esophageal	Female	58	Upper thoracic esophageal cancer with mediastinal lymph node metastasis
T6	Thymus	Female	64	Thymic carcinoma with metastasis to the sternum and left sacrum
H1	Health	Female	60	None
H2	Health	Female	45	None
H3	Health	Female	28	None
H4	Health	Female	50	None

H5	Health	Female	36	None
H6	Health	Female	56	None

Tab. S3 Capture efficiency of in the samples with different concentration of sEVs.

Amount (μg)	1	2	3	Average	Captured	Capture efficiency (%)
1	2.50E+09	2.40E+09	2.90E+09	2.60E+09	7.00E+08	21.21
2	2.50E+09	2.70E+09	2.30E+09	2.50E+09	8.00E+08	24.24
4	2.00E+09	1.80E+09	2.00E+09	1.93E+09	1.37E+09	41.41
8	7.80E+08	7.20E+08	9.20E+08	8.07E+08	2.49E+09	75.56
10	4.70E+08	3.30E+08	3.70E+08	3.90E+08	2.91E+09	88.18
15	3.30E+08	3.20E+08	3.70E+08	3.40E+08	2.96E+09	89.69

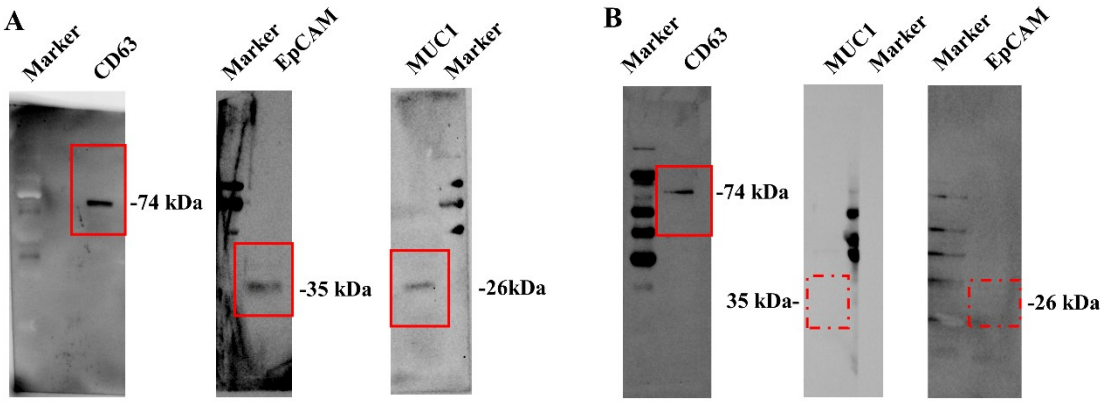

Fig. S1. The raw data from the western blotting experiments demonstrating the expression of one sEVs' marker and two breast cancer-related markers on (A) MCF-7 sEVs and (B) B16 sEVs.

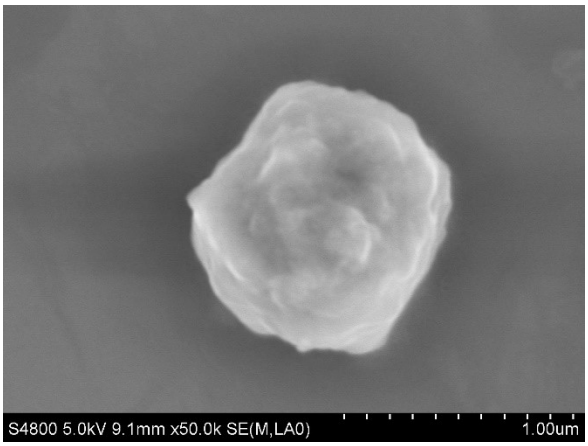

Fig. S2. SEM image of the streptavidin functionalized magnetic beads (SA-MBs).

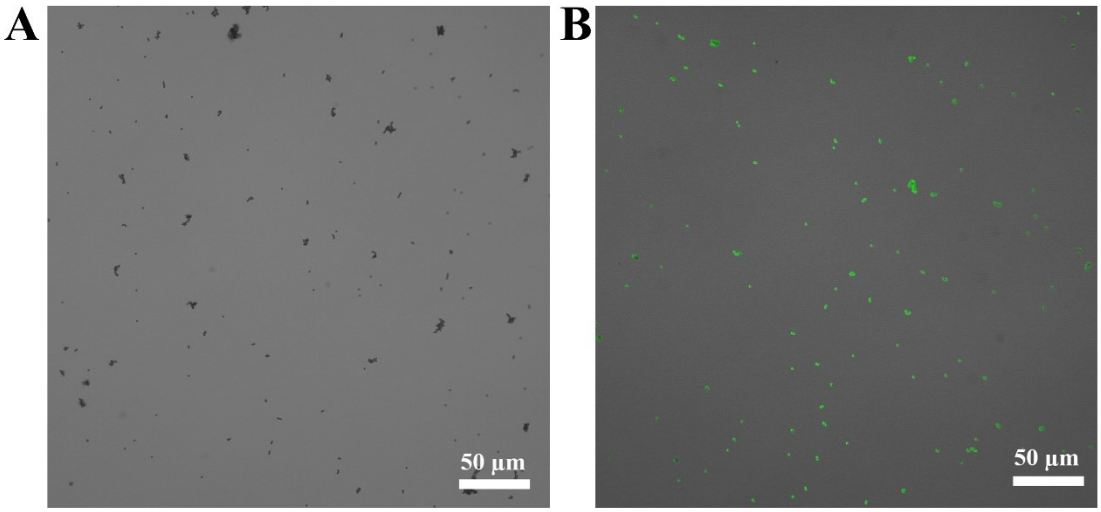

Fig .S3. CLSM images of FAM-labeled secondary antibody incubated with either (A) SA-MBs or (B) IMBs.

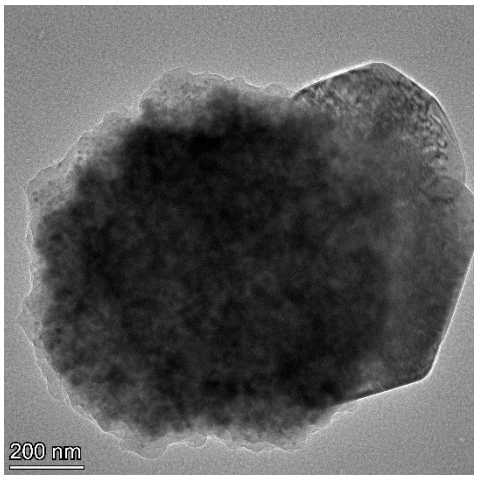

Fig. S4. TEM image of the streptavidin functionalized magnetic beads.

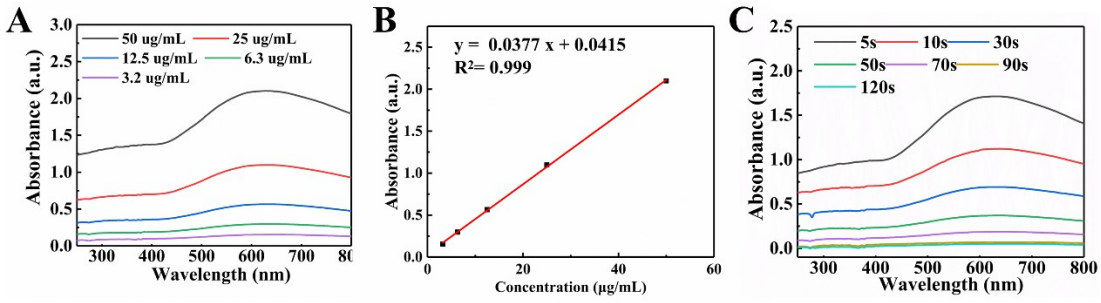

Fig. S5. (A) UV-vis absorbance spectra and (B) linear relationship showing the maximum absorbance at 632 nm of IMBs with varied concentrations. (C) UV-vis absorbance spectra of IMBs after isolation magnetically at different time points.

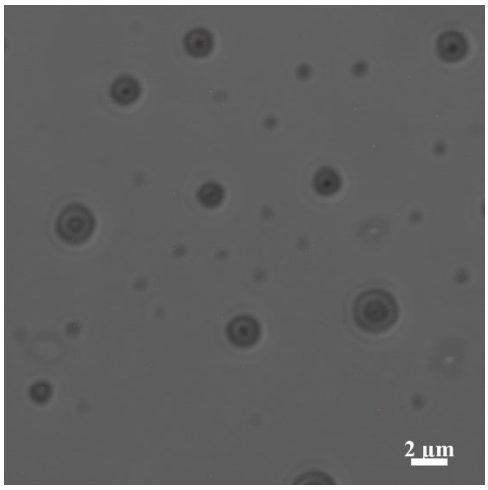

Fig. S6. CLSM image of SA-MBs incubated with PKH26-stained sEVs.

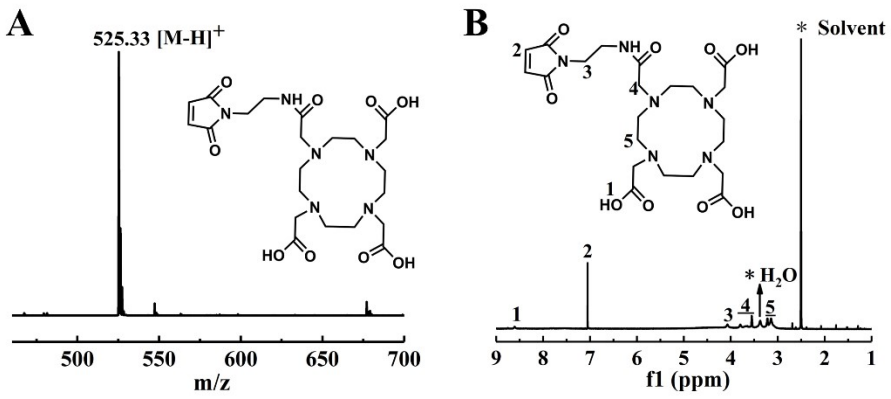

Fig. S7. (A) MALDI-TOF-MS spectrum of Mal-DOTA. Anal. Calcd for Mal-DOTA ($C_{22}H_{34}N_6O_9$): C, 50.18; H, 6.15; N, 15.96; O, 27.35. MALDI-TOF-MS results for PTTA, m/z 525.33, $[M-H]^+$. (B) ^{1}HNMR spectrum of Mal-DOTA (400 MHz, DMSO-d_6, room temperature): δ (ppm) 3.14-3.22 (m, 16 H), 3.55-3.79 (t, 8H), 4.07 (s, 2H), 7.05 (s, 2H), 8.61 (s, 3H).

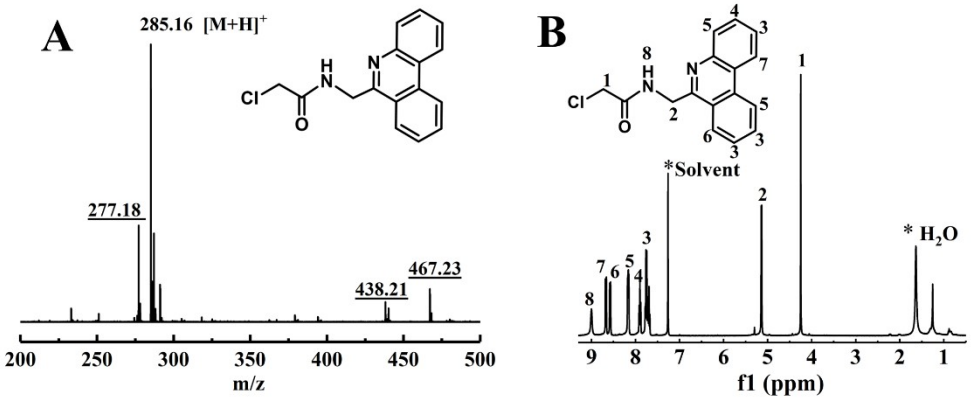

Fig. S8. (A) MALDI-TOF-MS spectrum of Cl-PA. Anal. Calcd for Cl-PA ($C_{16}H_{13}ClN_2O$): C, 67.49; H, 4.60; Cl, 12.45; N, 9.84; O, 5.62. MALDI-TOF-MS results for PTTA, m/z 285.16, $[M-H]^+$. (B) ^{1}HNMR spectrum of Cl-PA (400 MHz, DMSO-d_6, room temperature). 4.24 (s, 2H), 5.13 (d, 2H), 7.76 (s, 3H), 7.89 (m, 1H), 8.16 (s, 2H), 8.56 (m, 1H), 8.66 (q, 1H), 8.99 (s, 1H).

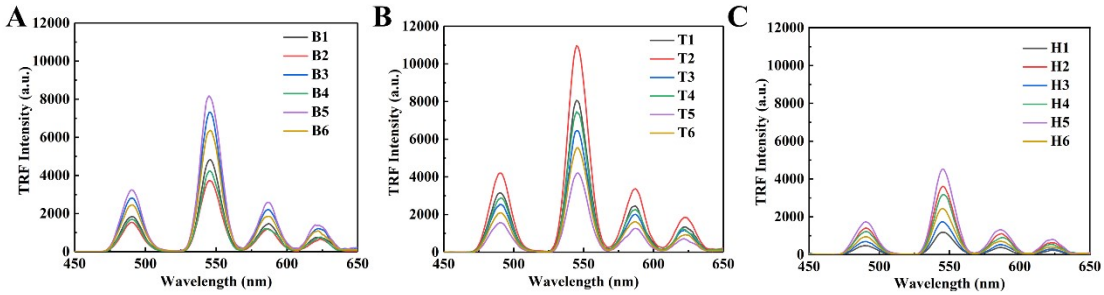

Fig. S9. The detection results of ALL strategy applied in human plasma samples from (A) Epithelial breast cancer, (B) Other epithelial cancers and (C) Healthy volunteers.

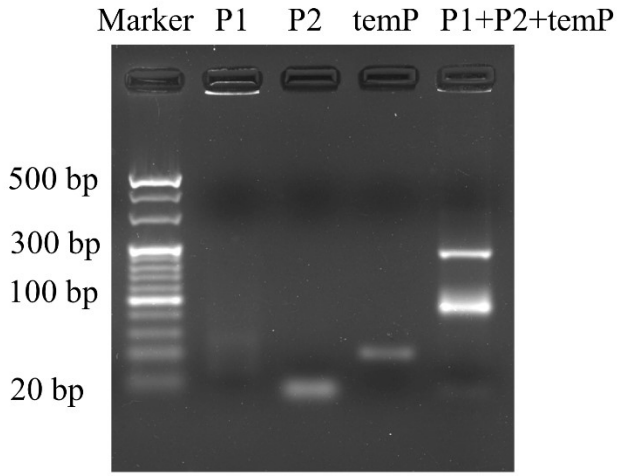

Fig. S10. Agarose electrophoresis to verify the feasibility of temP recognition.

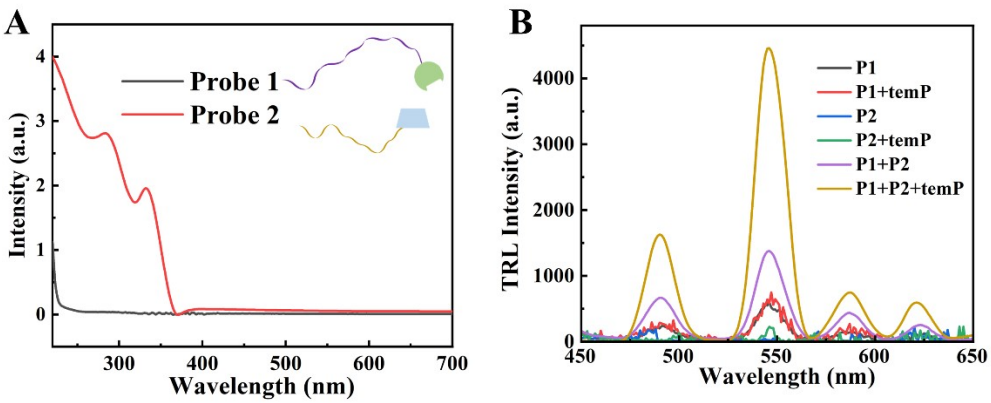

Fig. S11. (A) UV-vis spectra of P1 and P2, (B) TRL spectra of the designed probe precursor complexes or mixtures.

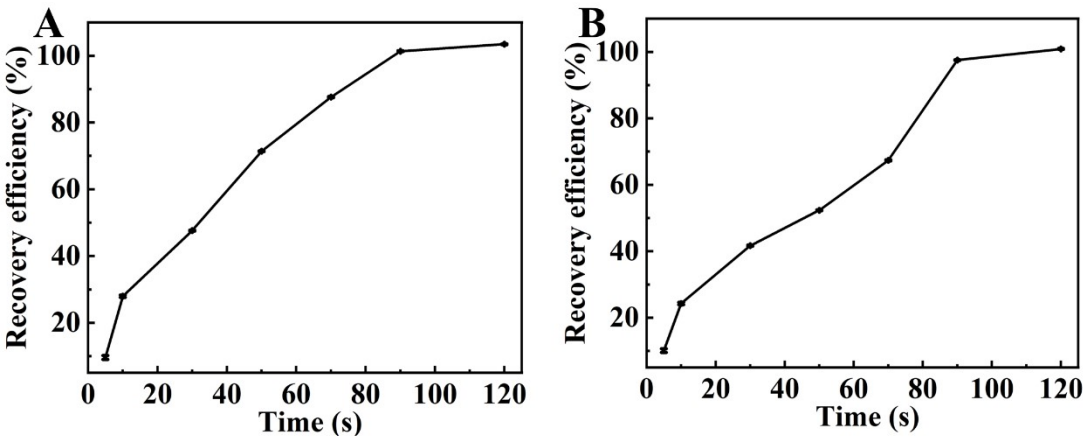

Fig. S12. Recovery efficiency of (A) IMBs@sEVs and (B) IMBs@sEVs@P1+P2.